8th International Conference on Behavior of Steel Structures in Seismic Areas
Shanghai, China, July 1-3, 2015

COLUMN BASE WEAK AXIS ALIGNED ASYMMETRIC FRICTION CONNECTION CYCLIC PERFORMANCE

J. Borzouie*, G.A. MacRae* , J.G. Chase, G.W. Rodgers**, G.C. Clifton*****

* University of Canterbury, Department of Civil and Natural Resources Engineering, New Zealand.
e-mails: jamaledin.borzouie@pg.canterbury.ac.nz, gregory.macrae@canterbury.ac.nz
** University of Canterbury, Department of Mechanical Engineering, New Zealand.
e-mails: geoff.chase@canterbury.ac.nz, geoff.rodgers@canterbury.ac.nz
***University of Auckland, Department of Civil and Environmental Engineering, New Zealand.
e-mail: c.clifton@auckland.ac.nz

Keywords: Asymmetric Friction Connection, WAFC, Low Damage Design

Abstract.

Abstract. *Recent low damage studies have been made on beam-to-column joints and braces. However, if there is significant yielding damage at the column bases, even with no upper structure damage, then the whole structure may need replacement. Therefore, there is a need to develop low damage base connections. This paper presents experimental tests of columns connected to base plate by weak axis aligned asymmetric friction connection (WAFC base) to evaluate if it performs as a low damage connection. Cyclic tests are conducted in-plane about the strong axis, and out-of-plane with and without applied axial force to drift ratios as high as 4%. Observations from the experimental tests demonstrate that this type of base connection can tolerate high levels of drift without any significant damage at the base. Some flange compressive yielding occurs especially when the column was subjected to axial force. Generally, no major damage happened which interrupt the performance of the column and the base connection, and it can be categorized as a low-damage connection. Also, the presented analytical model for estimation of WAFC performance provides a reasonable estimation of the experimental results.*

1 INTRODUCTION

The development of seismic design criteria is an on-going process. Recently, a new low damage design approach has emerged, with a main design objective to maintain life safety while reducing structural damage, and the associated cost and down time. This approach dissipates energy in replaceable elements rather than sacrificial damage to the structural frame. Studies on "low damage" construction in steel frame structures has focused on beam to column moment resisting joints [1,2,3,4], braces [5], and developing rocking steel frame [6] that have been used in real construction [7]. However, no study has focused on low damage base connections.

If all the low damage structural elements remain un-damaged after an event, but the base of the structure experiences damage, replacing the base plate is not practical due to its position under high axial load. Moreover, any residual deformation at the base can cause large residual displacement at the top storeys. Therefore, there is a need to develop novel detailing and methods for the base connection that can sustain higher demands with low or no damage.

This paper describes experimental tests of a column base weak axis aligned asymmetric friction connection (WAFC base) to:

(i) evaluate whether it can be considered a low damage connection considering the modes of deformation involved under (a) in-plane loading (b) out of plane loading with and without axial force.

(ii) present a simple analytical model for evaluation of its performance

2 METHODOLOGY

2.1 Detailing of WAFC

The column base weak axis aligned asymmetric friction connection (WAFC base), which is detailed in Figure 1, uses asymmetric friction connection (AFC) to connect column and the base plate. The column and the base plate are in full contact, but without direct welding, and are connected by four AFC. In each AFC, one plate is welded to the column (*column plate*) and a steel plate with oversized rounded holes welded to the base plate (*flange plate*). The oversized holes in the flange plate allow considerable rotation of the column end relative to the base plate. Since the column deforms in two directions, the round holes in the flange plate provide space for bending in both directions. Bisalloy500 shims are placed on all sliding surfaces to their high hardness and abrasion resistance. Finally, the cap plate is placed on the inside of the flange plate. The cap plate is the floating plate that is connected to the rest of the joint with bolts. All plates are connected with high strength bolts (Grade 8.8). The flange plate, shims and cap plate are placed at a distance labelled "*Cl A*" from the column face. This distance should be sufficient to prevent contact between the flange plate and column and prevent excessive demand on the column or flange plate under large rotations. "*Cl B"* is placed to prevent contact of the column plate, shims, and cap plate with the base plate, as it can increase demands of the column plate.

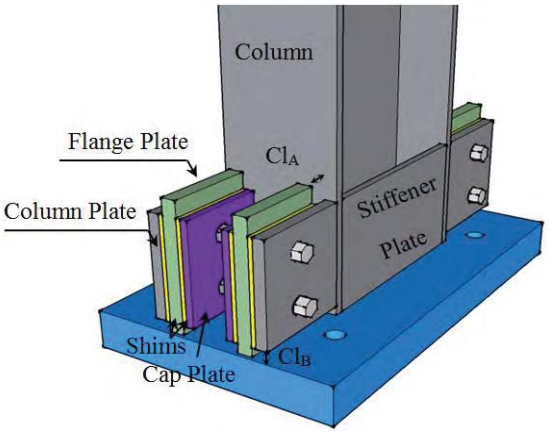

Figure 1: WAFC Base

The mechanism of sliding for this base connection when the column bends about the strong axis is as follows. The column starts from its at-rest condition. When the base moment becomes equal to the resisting moment of the friction connection with one shear plane, the column plates start sliding. At this stage the cap plate does not slide because the shear force is not enough for cap plate sliding. Also, shear and flexural stiffness of the bolts contribute to base rotational stiffness. As top displacement of the column is increased, the bolts move on an angle and pull the cap plate and allowing it to slide. The shear force is twice the required shear for sliding in only one shear plane. Moreover, all of the column and cap plates start sliding and the rotational stiffness at the base is equal to zero. When the load is reversed, slip initially occurs in only one shear plane between the flange plate and the column plat. For larger reverse deformation, sliding occurs in both sides of the flange plate, and rotational stiffness is equal to zero.

Under column weak axis bending the main difference compared to strong axis bending is the additional prying effect of the flange plates as the column rotates about a point near the flange.

2.2. Experimental Program

Figure 2a,b shows the experimental setup. Here, actuator A, pushes in the east-west direction causing bending about the column strong axis. Two others, actuators B and C, push in the north-south direction causing weak axis bending. They are programmed to allow strong axis deformation without moving the specimen out-of-plane during these tests, and prevent twist. Three rotary potentiometers positioned parallel to each actuator are used to monitor and control displacement. A hydraulic jack with a ball bearing joint was placed on top of the column for tests with axial force to apply an axial force of 320 *kN*, equal to 20% of the column section axial capacity ($0.2\phi AF_y$). The force was kept constant through the lateral deformations, and it was recorded by two load cells placed on top of a SHS section cross-beam above a jack measured the axial force. The tested WAFC configuration is detailed based on section 2.1 as shown in

Figure 2c.

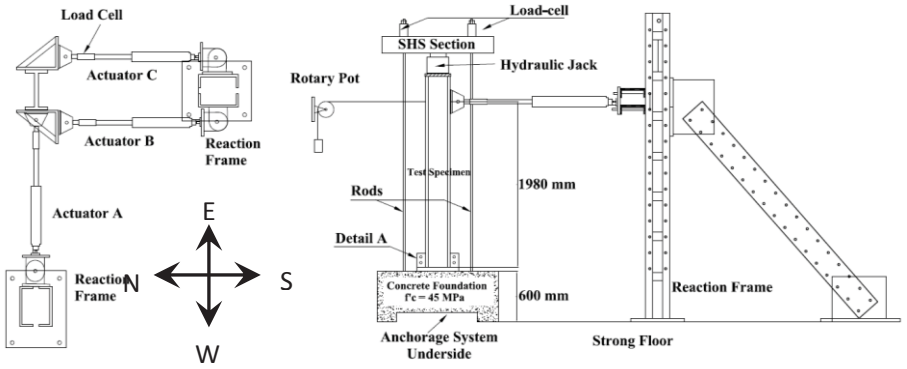

a. Plan b. Elevation

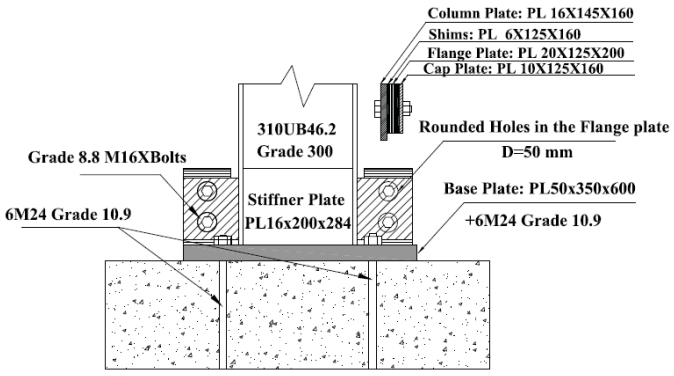

c. Detail of base connection (Detail A)

Figure 2: Experimental test set-up

To obtain comprehensive understanding of this base connection, four specific cyclic tests were conducted as shown in Table 1 that is sorted based on the test order.

Table 1: Tests conducted

No	Axis of Bending	Axial force
1	Strong	Zero
2	Weak	Zero
3	Strong	320kN (0.20Ns)
4	Weak	320kN (0.20Ns)

2.3. Loading Regime

A cyclic loading regime according to ACI report T1.1-01 was applied to each specimen. Initial loading started from 0.2% drift (4 *mm*) and finished at 4% drift (80 *mm*). The increase in each new drift is 1.25 to 1.5 time that of the previous step.Three full cycles and one cycle of half of the drift level in the studied direction were applied as shown in Figure 3.

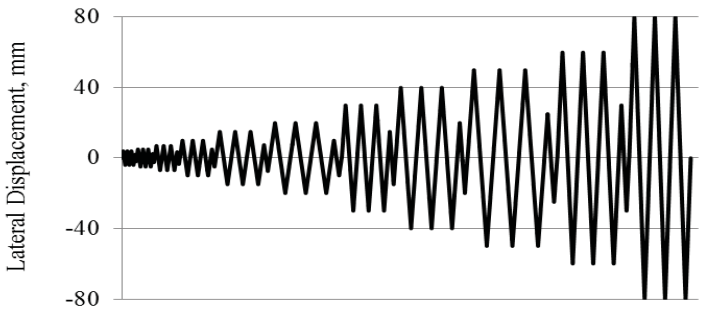

Figure 3: Test loading regime

2.4. Analytical Prediction

The nominal sliding force for each AFC bolt is given in Equation 1[2] where, F_s is sliding force of each bolt, μ is the friction coefficient, η is the number of shear planes, and N_{tf} is the proof load per bolt. The friction coefficient of steel on Bisalloy 500 was taken as 0.21[8].

$$F_s = \mu \times \eta \times N_{tf} = 0.21 \times 2 \times 95 = 40 kN \quad (1)$$

The maximum base moment from lateral loading causing strong axis bending, M_{Xbaseu}, is the sum of the sliding moment, M_{Slide}, and the moment from axial force, M_{Axial}, as given in Equation 2 where n_{Bolt} is number of the bolts in the AFCs on one side of the base connection, F_s is the sliding force in each bolt as defined in Equation 1, d is the horizontal distance of sliding bolts up to the neutral axis, and D_{Axial} is the perpendicular distance from the centre of axial force, P, to the neutral axis. Iteration is conducted on the neutral axis depth, c, until the area of the compression side of the section, all at the yield stress as is commonly assumed in plastic design, resists the axial force, N. Such an assumption is appropriate when the friction forces on either side of the neutral axis have similar magnitude but opposite directions. For weak axis bending, since only the AFCs in tension side slide, their sliding force should be added to the axial force for calculation of the neutral axis.

$$M_{xbaseu}=M_{slide}+M_{Axial}= (n_{bolt} \times F_s \times d) + (P \times D_{Axial}) \quad (2)$$

When the column bends about its weak axis, a prying moment, M_{Prying}, happened in addition to the moment resistance from the frictional sliding and axial force components, M_{Slide} and M_{Axial}. M_{Prying} mainly comes from bending of the column flange plates as given in Equation 3 where: L_1 is the distance from top of the column plate to the base plate; I_{fp} is the second moment of inertia about the weak axis of the flange plate; and L_2 is length of the column plate. This moment cannot be greater than the flange plate plastic flexural strength, $M_{P\text{-}fp}$, given by the Equation 4 where: b_{fp} is width of the flange plate; t_{fp} is flange plate thickness; and σ_y is the flange plate yield stress.

$$M_{Pr\,ying} = 2 \times \frac{\theta_{Base} \times 3EI_{fp}}{L_1^2} \times L_2 \tag{3}$$

$$M_{P-fp} = 2 \times \frac{\sigma_y \times b_{fp} \times t_{fp}^2}{4} \tag{4}$$

Column base rotation of the experimental test can be measured from base potentiometers according to Equation 5 where x_{UD} is the distance between potentiometers measuring tension and compression, Δ_{Up} and Δ_{Down} respectively, perpendicular to the neutral axis. The neutral axis depth from the experimental test, c, is given in Equation 6 where x_{cp} is the distance between the extreme fibre of the section and the position of the potentiometer measuring compression perpendicular to the neutral axis, Δ_{Down}. The uplift displacement at the extreme tension side of the specimen, Δ_{Uplift}, is again given by Equation 7 using the experimental definition of the neutral axis, where c_{Tens} is the distance perpendicular to the neutral axis to the extreme fibre of the section.

$$\theta_{Base} = \frac{\Delta_{Up} - \Delta_{Down}}{x_{UD}} \tag{5}$$

$$c = \frac{\Delta_{Down}}{\theta_{Base}} - x_{cp} \tag{6}$$

$$\Delta_{Uplift} = \theta_{Base} c_{Tens} \tag{7}$$

In each test, column base moment, M_{Base}, and column base rotation, θ_{Base}, were computed from the recorded lateral force and column lateral displacement. The solid bilinear curve shows the predicted performance according to the above method. It is assumed the base connection is rigid before sliding on the first surface and using M_{Xbase} from Equation 2 with η= 1 in Equation 1, and the cap plate slides at 4% drift for drawing the second line, with η= 2 in Equation 1.

3. RESULTS AND DISCUSSION

Maximum moment of WAFC that was bended about strong axis without axial force goes up to 34% of the plastic moment capacity of the column assuming yielding in tension and compression side (233 kN.m) due to the sliding as shown in Figure 4a. No paint flaking was observed in the column and boundary plates indicating that they remained elastic.

Experimental test parameters are compared with the predicted values of base moment in the X and Y directions, M_{base}; the position of the neutral axis, c; and column uplift, Δ_{uplift} for 4% drift, in Table 2.For test1, the base moment strength at 4% drift, was predicted to an accuracy of better than 7%. The depth of neutral axis, c, is zero because the friction devices on the different sides of the column have similar forces in compression and tension and there is no axial force on the specimen.

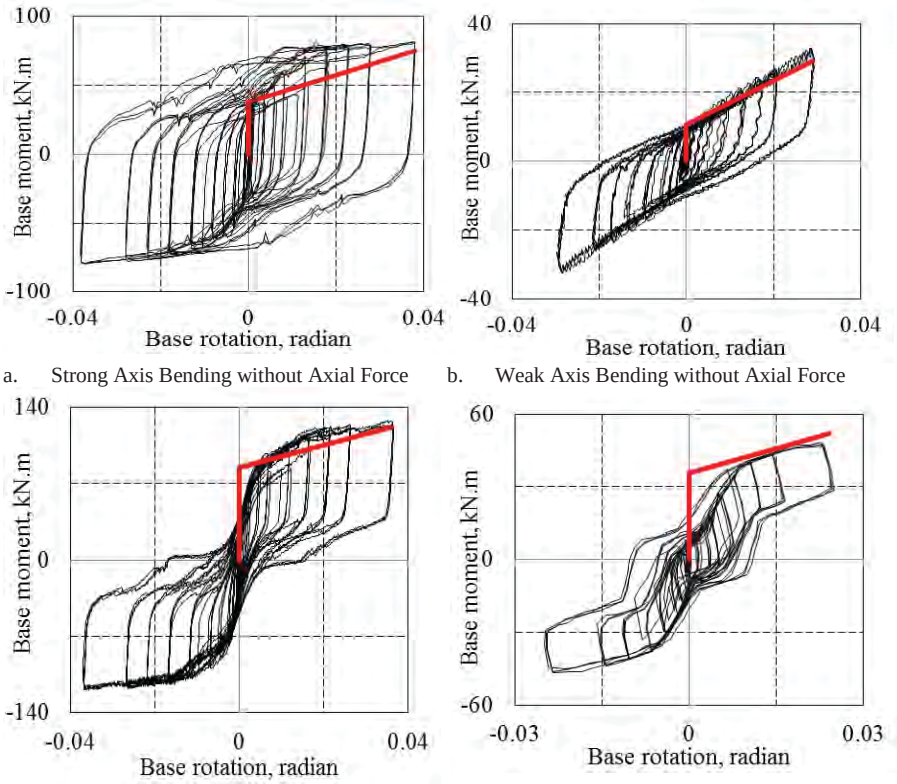

a. Strong Axis Bending without Axial Force b. Weak Axis Bending without Axial Force

c. Strong Axis Bending with Axial Force d. Weak Axis Bending with Axial Force

Figure 4: Moment- rotation of strong axis bending with and without axial force

Table 2: Predicted and Experimental Actions

No	Bending Axis	Axial Force	No. AFC bolts	$M_{X,base}$, (kN.m)		$M_{Y,base}$, (kN.m)		c (mm)		Δ_{uplift} (mm)	
				Pred[1]	Expt[1]	Pred	Expt	Pred	Expt	Pred	Expt
1	Strong	Zero	Four	75	80.5	0	0	0	0	11.6	12.05
2	Weak	Zero	Four	0	0	36	32.7	21[2] / 1.6[3]	12	4.9	4.3
3	Strong	320kN	Four	122	123.7	0	0	6	14	11	10.1
4	Weak	320kN	Four	0	0	52	47.4	42[2] / 3.2[3]	36	3.4	2.28

[1] Pred: predicted value, Expt: value obtained from experimental test
[2] Neutral axis of the column above stiffener plates
[3] Neutral axis of the column with stiffener plates

In the second test, the column bended about the weak axis without applying axial force. The maximum moment reaches 32.7 kN.m, which is 10% less than the column section nominal moment capacity of 35 kN.m for weak axis bending as shown in Figure 4b. No paint flaking observed in the column and boundary plates that shows elements remain elastic. The cap plates did not slide, but the column plates sliding was recorded. The quantified results in Table 2 show the described method can predict the M_{Base} and Δ_{Uplift} of the column for test 2 with the accuracy less than 12%. The sliding force in the tension side is considered for calculation of the neutral axis. Two values for position of neutral axis is calculated, *c*, since the stiffener plates did not extend in the whole height of the column. When stiffener plates are considered, *c* is equal to 1.6 mm and without stiffener plates, *c* is 21 mm. The actual position of the neutral axis is between these two values. Since no axial force was applied to the column after a few cycles the column moved up, and a gap appeared between the base plate and the column at zero displacement. Some plastic deformation at the column corners happened as the corner strain, which wash recorded by connected potentiometers to the column plates (4750×10^{-6}), was higher than yielding strain that is 1600×10^{-6}.

For WAFC that was bended about the strong axis with axial force, the maximum moment goes up to 64% of the nominal section flexural strength as shown in Figure 4c. The self-centring base moment from the axial force (47 kN.m) is smaller than sliding moment on both sides of the AFC (75 kN.m) but greater than sliding resistance on one side the AFC (37.5 kN.m). It shows, the applied axial force can provide self-centring for levels of drift up to sliding of the cap plate. However, for greater level of base moment, the static recentring cannot be provided. However, dynamic recentring after an earthquake shaking is likely [9].No yielding was observed in the column or any connection elements. The numerical results presented in Table 2 described the proposed method can predict M_{Base} of test 3 with 1% accuracy, and column uplift, Δ_{Uplift} ,was 9% less than predicted. The position of neutral axis in the first cycle of 4% drift was less than half of the calculated value. It shows the position of neutral axis is much closer to the column centre than predicted. The possible reason could be some local flange yielding that occurred in test 2. It caused reduction the amount of section in contact with the plate. Therefore, initial stiffness was reduced, and base uplift occurred at a lower base moment than predicted.

The previous yielding at the column from test 1 to 3 reduced the column area that contacted with the column. Therefore, column base uplift in test 4 occurred at about 10 kN.m which is about one-third of that predicted and at about one-half of that estimated for uplift considering axial force, of 21 kN.m as shown in Figure 4d. In tests 1 to 3, the column flange mainly yielded. Hence, the column flange tips did not contact the base plate for small base rotations. The predicted moment at 4% drift according to the mentioned method is higher than the column flexural capacity of 52 kN.m. Therefore this value was considered as the predicted value in Table 2. The column flange yielded from 3% drift as observed by paint flaking. For this axially loaded column bending about the weak axis, when the lateral force was reduced from the peak displacement, the rotation at the column base increased as shown in Figure 4d. This occurred even though the displacement at the loading point reduced because during this unloading the elastic displacement of the column alone started to decrease making the column become straighter. The effect of straightening, causing the base rotation to increase, was more significant than the effect of the decrease in displacement at the loading point, which causes the column base rotation to decrease. Greater amount of compressive yielding at the base of the column, and greater flexural/shear deformation of the column resulted in 47% reduction in the column uplift compare to test 2. The predicted neutral axis depth without stiffeners is 42 mm, and this length is equal to 3.2 mm considering the stiffeners. Since the stiffeners did not extend over full height of the column, the actual length lies between these two values. In this test, the neutral axis depth was 36 mm that is close to the value assuming no stiffeners.

4. CONCLUSION

This paper describes experimental testing of the column weak axis aligned asymmetric friction connection (WAFC) subject to strong axis, weak axis with and without axial force. It was shown that:

- The base connection did not have considerable strength degradation. However, some stiffness degradation due to flange yielding of the column was observed. The bolts and shims can be reused after an earthquake and level of shims degradation was minor. Also, the boundary plates remained elastic. Generally, no major damage was observed that interrupted the base and the column performance, and it can be categorized as a low damage base connection. If it is required any repair, it may be undertaken by retightening and replacing of the bolts and shims.
- A simple analytical model developed which can calculate the neutral axis of the column, column uplift, and the moment resistance at 4% drift. Frictional resistance, axial force effects and prying effects were considered in the analytical model. It can provide a reasonable estimate for strength. Also, for un-tested column it can predict the stiffness with acceptable accuracy. However, during cyclic loading for further tests some yielding happened on the column that reduced the stiffness from the predicted value during subsequent test.

ACKNOWLEDGMENT

The authors would like to acknowledge the MBIE Natural Hazards Research Platform (NHRP) for its support of this study as part of the Composite Solutions project. All opinions expressed remain those of the authors.

REFERENCES

[1] Clifton, C. G., "Semi-rigid joints for moment resisting steel framed seismic resisting systems." PhD thesis, University of Auckland, 2005

[2] MACRAE, G. A., Clifton, G. C., Mackinven, H., Mago, N., Butterworth, J. & Pampanin, S." The Sliding Hinge Joint Moment Connection." Bulletin of the New Zealand Society for Earthquake Engineering, 43, 10, 2010.

[3] Rodgers, G. W., Chase, J. G., Mander, J. B., Leach, N. C. & Denmead, C. S."Experimental Development, Tradeoff Analysis and Design Implementation of High Force-To-Volume Damping Technology." NZSEE Bulletin, 40, 35-48, 2007.

[4] Rodgers, G., Solberg, K., Mander, J., Chase, J., Bradley, B. & Dhakal, R."High-Force-to-Volume Seismic Dissipators Embedded in a Jointed Precast Concrete Frame." Journal of Structural Engineering, 138, 375-386, 2012.

[5] Chanchi , J. C., Xie, R., MacRae, G., Chase, G., Rodgers, G. & Clifton, C. "Low-damage braces using Asymmetrical Friction Connections (AFC)." NZSEE. Auckland, New Zelaand, 2014.

[6] Clough, R. W. & Huckelbridge, A. A "Preliminary experimental study of seismic uplift of a steel frame" Berkeley: Earthquake Engineering Research Center, University of California, 1977.

[7] Latham, D., Reay, A. & Pampanin, S."Kilmore Street Medical Centre: application of a post-tensioned steel rocking system." Proc., Steel Innovations Conf, 2013.

[8] Chanchi, J. C., Macrae, G. A., Chase, J. G., Rodgers, G. W. & Clifton, C. G.. "Behaviour of Asymmetrical Friction Connections using different shim materials." NZSEE Conference, 2012.

[9] Macrae, G. A."P-Δ Effects on Single-Degree-of-Freedom Structures in Earthquakes." Earthquake Spectra, 10, 539-568, 1994.